Cosmological measurement of the gravitational constant G using the CMB, BAO, and BBN

B. Lamine, Y. Ozdalkiran, L. Mirouze, F. Erdogan, S. Ilic, I. Tutusaus, R. Kou, A. Blanchard

A&A, 697, A109 (2025)
https://doi.org/10.1051/0004-6361/202451602

Astronomy & Astrophysics

Cosmological measurement of the gravitational constant G using the CMB, BAO, and BBN

B. Lamine[1,⋆], Y. Ozdalkiran[1], L. Mirouze[1], F. Erdogan[1], S. Ilic[2], I. Tutusaus[1], R. Kou[1,3], and A. Blanchard[1]

[1] Institut de Recherche en Astrophysique et Planétologie (IRAP), Université de Toulouse, CNRS, UPS, CNES, 14 Av. Edouard Belin, 31400 Toulouse, France
[2] Université Paris-Saclay, CNRS/IN2P3, IJCLab, 91405 Orsay, France
[3] Department of Physics & Astronomy, University of Sussex, Brighton BN1 9QH, UK

Received 22 July 2024 / Accepted 26 March 2025

ABSTRACT

Recent cosmological observations have provided numerous new observations with an increasing level of precision, ushering in an era of precision cosmology. The exquisite quality of these observations opens up new possibilities in terms of measuring fundamental constants with good precision on scales that are complementary to laboratory references. In particular, the cosmic microwave background (CMB) temperature and polarisation spectra contain a wealth of information that goes well beyond the basic cosmological parameters. In this paper, we update the precision on a cosmological determination of the gravitational constant, G, by using the latest Planck data release (PR4) in combination with the latest baryon acoustic oscillation (BAO) from the Dark Energy Spectroscopic Instrument (DESI) data release 1 and the BBN prior on the primordial helium fraction. We demonstrate a precision of 1.8%, corresponding to a ∼40% improvement with regard to previous results in the literature. This is comparable to the level achieved by Cavendish in 1873 using a torsion balance. However, it is a complementary measurement because it has been obtained under wildly different physical environments compared to laboratory results or even studies of the very nearby Universe. Our analysis takes into account the modification of the primordial helium fraction predicted by Big Bang nucleosynthesis (BBN), induced by a variation in G. We also point out the importance of the polarisation data in attaining the ultimate level of precision. In particular, we discuss the constraints that can be obtained by considering either the low-ℓ or the high-ℓ part of the spectra. Within the ΛCDM model, we find $G = (6.75 \pm 0.12) \times 10^{-11}\, m^3\, kg^{-1}\, s^{-2}$. This measurement is compatible with laboratory results within one standard deviation. Finally, we show that this cosmological measurement of G is robust against several assumptions made on the cosmological model, particularly when considering a non-standard dark energy fluid or non-flat models.

Key words. gravitation – cosmic background radiation – primordial nucleosynthesis

1. Introduction

Even though it stands as the oldest fundamental constant of our standard model, the gravitational constant, G, has not been used to define the kilogram in the new international system of units BIPM (2019). The Planck constant, h, (not to be confused with the reduced Hubble constant) has instead been selected and fixed at a specific value. Consequently, the gravitational constant must be determined experimentally and, unfortunately it remains the least precisely measured fundamental constant. This enigma can be readily attributed to the exceptionally feeble nature of the gravitational force when compared to the other fundamental forces in the Universe. Therefore, we rapidly arrive at scenarios in which non-gravitational effects surpass the relevant gravitational effect when we are trying to measure G with a high level of precision and accuracy. According to the Committee on Data for Science and Technology (CODATA 2018), laboratory experiments enable us to measure Newton's gravitational constant as: $G_{\rm codata} = 6.674\,30(15) \times 10^{-11}\,{\rm m^3\,kg^{-1}\,s^{-2}}$, with a relative uncertainty of (only) 2.2×10^{-5} (Tiesinga et al. 2021). Moreover, these laboratory measurements suffer from not yet completely understood terrestrial effects that affect the final precision of G (Fixler et al. 2007; Anderson et al. 2015; Xue et al. 2020), making an independent measurement of G at cosmological scales an intriguing undertaking.

To achieve a high-precision measurement of G, it is imperative to consider physical experiments where non-gravitational effects are effectively under control and where gravitational forces assume a prominent role. This allows us to disentangle non-gravitational contributions from their gravitational counterparts (Uzan 2003, 2011). Interestingly enough, this is a situation that can be seen in cosmology during the baryon-photon plasma phase before recombination, where both the gravitation effects and Thomson scattering of photons by electrons are present (Zahn & Zaldarriaga 2003). Indeed, the physics involved during this period are supposedly well understood, as illustrated by the very good fit of our theoretical model to the measurements of the cosmic microwave background (CMB) temperature and polarisation spectra, as well as all the internal consistency checks that can be performed (Planck Collaboration VI 2020). In particular, it is quite remarkable to realise that the temperature of the CMB itself can be inferred solely from its fluctuation spectrum, as demonstrated in Ivanov et al. (2020). Since the physics of recombination involve both non-gravitational and gravitational physics, this allows us to obtain a sensitivity to G that is not degenerate with other parameters, such as the energy densities. Therefore, cosmological measurements of G using the CMB have been performed in the literature, either from (phenomenological) model-independent

⋆ Corresponding author: brahim.lamine@irap.omp.eu

studies (Zahn & Zaldarriaga 2003; Umezu et al. 2005; Chan & Chu 2007; Galli et al. 2009; Bai et al. 2015; Wang & Chen 2020; Sakr & Sapone 2022) or based on specific models, such as scalar-tensor theories (Riazuelo & Uzan 2002; Nagata et al. 2004; Ballardini et al. 2022; Braglia et al. 2020; Ooba et al. 2017). Even if these approaches are not competitive with respect to laboratory measurements, a cosmological determination of G is complementary in terms of scales. Indeed, many extended models of general relativity (GR) predict either a (space-)time variation in this constant at cosmological scales (the reference model being the Jordan-Brans-Dicke model, Jordan 1959; Brans & Dicke 1961; Peracaula et al. 2020) or a different value for different spatial scales (Bertschinger & Zukin 2008). Some screening mechanisms allow us to recover the laboratory measurements (Joyce et al. 2015). In particular, if the gravitational constant inferred from cosmology turns out to be different from the local one, this would point towards a modification of gravity at large scales. Finally, testing the value of G in extreme conditions, such as those at the very beginning of the Universe, where the energy content is dominated by radiation, is also extremely interesting.

This paper presents updated constraints on a cosmological measurement of the gravitational constant G. Our focus is specifically on high-redshift probes, and we exclude type-Ia supernovae (SNIa) data from our analysis. This exclusion stems from the ongoing debate surrounding the influence of the gravitational constant on the intrinsic luminosity of SNIa. Indeed, the straightforward expectation is that variations in G would affect the intrinsic luminosity due to its presumed correlation with the Chandrasekhar mass, $M_{\rm Ch}$, which is itself proportional to $G^{-3/2}$. Consequently, an increase in G would result in a diminished intrinsic luminosity (Gaztañaga et al. 2001; Garcia-Berro et al. 2006; Mould & Uddin 2014; Zhao et al. 2018). However, a study presented in Wright & Li (2018) (confirmed in Ruchika et al. 2024) was focussed on a comprehensive examination of the impact of altering the gravitational constant on SNIa. Utilising semi-analytical models, these authors discovered that when accounting for both the aforementioned effect and the standardisation procedure, where the light curve is stretched to match a predefined template, the net effect of increasing the gravitational constant G is to amplify the peak luminosity. This result runs counter to the initial intuitive expectation. Therefore, we have chosen to narrow our focus exclusively to high-redshift probes, given the uncertainties associated with SNIa measurements in the context of varying G.

Here, we consider the latest PR4 analysis of Planck data (Tristram et al. 2024), which represents an improvement with respect to Planck 2018 (Planck Collaboration VI 2020). We use the term P20 to refer to this PR4 data analysis, while P18 refers to Planck 2018. Combining the latest baryon acoustic oscillation (BAO) data from DESI and a BBN prior for the primordial helium fraction $Y_{\rm He}$ from Olive (2021), we demonstrate a 1.8% percent precision in the determination of G. This value is compatible with laboratory measurements within one standard deviation; thus, our results do not indicate any modification of our gravitational laws at large scales. The addition of the BAO measurements only marginally improves the constraint on G, except when considering non-flat ΛCDM models. Our analysis properly takes into account the modification of the primordial helium fraction predicted by Big Bang nucleosynthesis (BBN) due to the variation in G. We also point out the importance of the polarisation data in the final precision, fostering the need for next-generation polarisation measurements such as those be provided by LiteBIRD (LiteBIRD Collaboration 2023) or CMB-S4 (Abazajian et al. 2019) experiments from the ground in the future, including the South Pole telescope (SPT)-3G (Benson et al. 2014) and the Simons Observatory (Ade et al. 2019). We also discuss the constraints that can be obtained by considering either the low-ℓ or the high-ℓ part of the spectrum. Finally, we show that this cosmological measurement of G is robust against several assumptions made on the cosmological model, particularly when considering a non-standard dark energy fluid or non-flat models. This is particularly important in the context of the slight internal tension in the Planck 2018 data concerning the flatness of the universe (Handley 2021; Di Valentino et al. 2020) or with the recent evidence by the combination of CMB and BAO measurements from the Dark Energy Spectroscopic Instrument (DESI) of evolving dark energy (DESI Collaboration 2025).

In Sect. 2, we briefly discuss how the gravitational constant affects the temperature and polarisation power spectra of the CMB. The methods and results are presented in Sect. 3, where we discuss our measurements of the gravitational constant and show that the cosmological model assumptions have no significant impact on the inferred value of G. We present our conclusions in Sect. 4.

2. Effect of changing the gravitational constant in the CMB anisotropies and light element abundances (BBN)

In this section, we characterise the effect of changing the gravitational constant G in the CMB spectra, both in temperature and polarisation. For convenience and in accordance with the literature, we define a free parameter λ_G such that $G = \lambda_G^2 G_{\rm codata}$. The first Friedmann-Lemaître equation is thus expressed as:

$$H^2 = \frac{8\pi\lambda_G^2 G_{\rm codata}}{3}\sum_i \rho_i, \tag{1}$$

where ρ_i is the energy density of a species, i. This model is denoted λ_GΛCDM. We note that the energy density of radiation, ρ_γ, is fixed by the temperature of the CMB obtained by FIRAS Fixsen (2009), $\rho_\gamma = \frac{8\pi^5 k_{\rm B}^4 T_{\rm CMB}^4}{15h^3c^3}$. The other densities are free parameters to be fixed by cosmological observations, along with the other usual cosmological parameters such as the Hubble constant. The Hubble factor, H, is clearly proportional to λ_G, which has led many authors to look to a potential solution of the Hubble tension based on a modification of G (Sakr & Sapone 2022). Unfortunately, these solutions have failed due to the exquisite constraints imposed by the CMB, as we discuss below.

It has already been pointed out in previous studies that gravity has no preferred scale. Therefore, when considering only gravitational effects, modifying G can be reabsorbed into a rescaling of the wavevectors (Zahn & Zaldarriaga 2003). Since the initial power spectrum of primordial perturbation is assumed to be a power law of $P_i(k) = k^{n_{\rm s}-1}$, a change in G would then be reabsorbed in the amplitude of initial primordial fluctuations and, eventually, the spectral index, $n_{\rm s}$ (Wang & Chen 2020); therefore no net influence of G would be left in the physical observables. Fortunately, non-gravitational physical processes are also at play during recombination, in particular, the Thomson scattering of photons on electrons. The effect of G could then be seen in the interplay between the expansion rate, $H \propto \lambda_G$, and the Thomson interaction rate, $\dot{\kappa}(z) = an_{\rm e}\sigma_{\rm T}$, where a is the scale factor, $n_{\rm e}$ is the free electron number density, and $\sigma_{\rm T}$ is the Thomson cross section. The CMB spectra are sensitive to

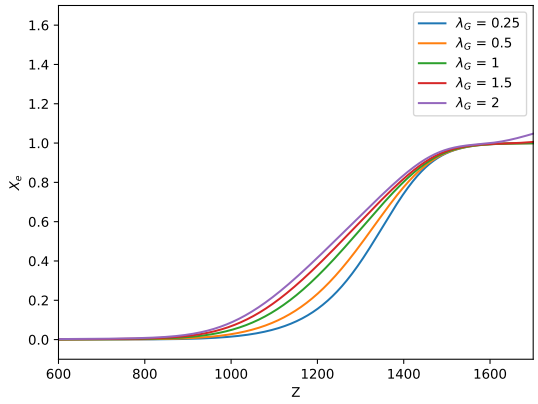

Fig. 1. Evolution of the ionisation fraction $x_e(z)$ with respect to the redshift, for different values of λ_G and fixed physical densities. We see that increasing G delays the time of recombination.

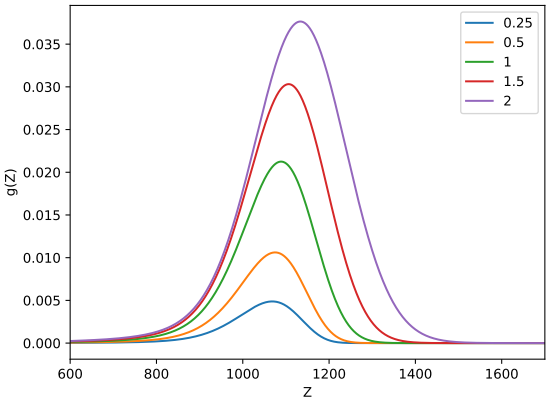

Fig. 2. Evolution of the visibility function with respect to the redshift, for different values of λ_G and fixed physical densities. The redshift of decoupling (defined as the maximum of the visibility function) increases when λ_G increases, so decoupling happens earlier. The width of the decoupling also increases with λ_G.

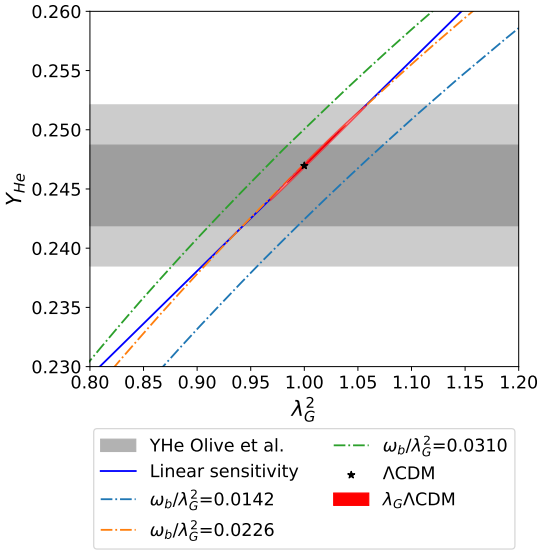

Fig. 3. Primordial helium fraction $Y_{\rm He}$ as a function of λ_G^2. For each curve, the baryon physical density, $\rho_{\rm b}$, which is proportional to $\omega_{\rm b}/\lambda_G^2$, has been kept constant while λ_G varies. The grey band indicates the observational constraints of Olive (2021). The black star is the best-fit standard ΛCDM model, while the red ellipse corresponds to the contour for the λ_GΛCDM model fitted with CMB + BAO from DESI + BBN. We observe that this contour is highly degenerate in the direction of constant physical density. The blue curve corresponds to the linear sensitivity model of Dent et al. (2007).

the ratio $\dot{\kappa}(z)/H(z)$. Therefore, a change in the expansion rate via a change in G, without accordingly changing the Thomson rate, will leave an impact on the CMB (Greene & Cyr-Racine 2023). More precisely, it has been shown in Galli et al. (2009) that increasing G delays the time of recombination and increases the duration of recombination , as can be seen from the evolution of the ionisation fraction shown in Fig. 1. That is because the expansion rate would be higher, making it more difficult for electrons to recombine with protons to produce hydrogen. At the same time, increasing G advances the moment of decoupling by raising the redshift corresponding to the peak of the visibility function, as well as broadening its width (see the Fig. 2 and also Rich (2015)). This effect on $g(z)$ contrasts with the effect on $x_e(z)$. Nevertheless, we note that those effects are rather small, since, for example, multiplying G by a factor of 4 only increases the decoupling redshift by 5%.

The same argument also holds for the BBN, since the predicted amount of light elements crucially depends on the comparison between the expansion rate, H, and nuclear reaction rates. Notably, a modification of the expansion rate, H, changes the time at which various weak and nuclear processes freeze-out. Specifically, the $p + n \longleftrightarrow D + \gamma$ reaction experiences earlier freeze-out if H increases (which could be the case if e.g. $\lambda_G > 1$). Consequently, it leads to an excessive production of deuterium and then helium, when compared to the scenario with $\lambda_G = 1$. This is why BBN can independently serve as a valuable tool for estimating the gravitational constant, as discussed in Accetta et al. (1990), Copi et al. (2004), Cyburt et al. (2005), Bambi et al. (2005), Alvey et al. (2020). As an illustration, Fig. 3 represents the effect of changing G on the primordial helium fraction $Y_{\rm He}$ (similar results as in Alvey et al. 2020), for a fixed physical energy density of baryons. In this figure, we represent the linear model of evolution of G from Dent et al. (2007), as well as our result stemming from the modified version of the CMB code PArthENoPE (Gariazzo et al. 2022). We see that the linear model (labelled as the linear sensitivity in Fig. 3) agrees well with our result, as we would expect. We also remark that the linear approximation of Dent et al. (2007) is clearly sufficient for our study.

Regarding the CMB temperature spectrum, the increase in the recombination duration results in an increase in the damping of the CMB peaks at small scales (characterised by large values of ℓ). This phenomenon arises due to the propagation of light between hot and cold regions, which tends to homogenise the temperature through the effect of viscosity and heat conduction, thereby causing a dampening of the CMB peaks. Small angular scales exhibit a more pronounced impact due to the fact that during the recombination phase, light is capable of traversing these smaller scales, facilitating the heat conduction over them. Conversely, larger scales characterised by wavelengths greater than the distance covered by light throughout the recombination phase do not permit significant heat conduction effects. This effect can readily be seen in the temperature power spectrum of the CMB represented in Fig. 4. In this plot, the first peaks have been appropriately normalised to facilitate a straightforward comparison of damping behaviours across various values of λ_G. These curves have been plotted using the same physical

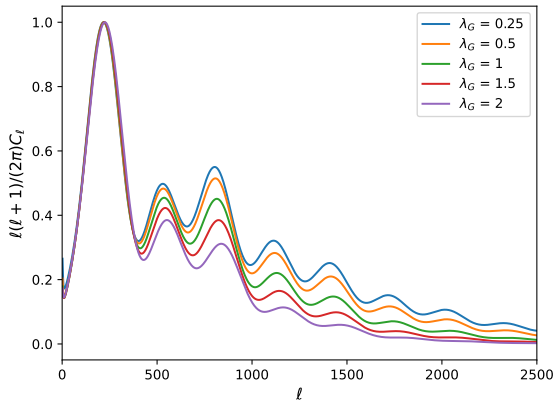

Fig. 4. Effect of λ_G on the temperature power spectrum of the CMB. The first peak has been normalised (in the amplitude of the first pic) and the same physical energy densities have been used for each curve. This plot shows the increase in the damping tails with increasing λ_G.

energy densities ρ_i (which necessitates a different value for H_0 to ensure that $\sum_i \Omega_i = 1$). We can clearly observe that higher values of λ_G indeed lead to an intensified damping of the peaks at small scales (high ℓ). This phenomenon forms the basis for extracting the gravitational constant G from the CMB temperature power spectrum. More precisely, we may extract the damping scale, k_D, from the temperature spectrum, and subsequently compare it to its anticipated value. This expected value is in fact the geometric mean of the horizon size and the mean-free path (Hu et al. 1997), both of which can also be independently extracted from the CMB peaks. The consistency between the observed and expected relationship not only serves as a robust consistency check for CMB data (Hu et al. 1997) but also contributes significantly to the accuracy of the gravitational constant G measurement and its accordance with the standard CODATA value $G_{\rm codata}$.

Nonetheless, the impact observed in the temperature spectrum alone does not yield a highly precise measurement of the gravitational constant G. This is evident in Table 1 and Fig. 11, which present constraints derived from the temperature anisotropy (TT) component of the spectrum (see a detailed discussion in the section on our results). Fortunately, the effect of changing the value of G on the polarisation power spectrum (EE) shows an interesting feature that physically justifies the usefulness of combining the polarisation data with the temperature data to significantly enhance the precision on the measurement of G (see Table 1). Specifically, apart from the previously described heightened damping of quadrupolar anisotropies at small scales as λ_G increases, there is a concurrent global amplification of quadrupole anisotropies. This occurs because light propagates over longer distances (since the recombination duration increases with λ_G), resulting in higher level of polarisation (Zaldarriaga & Harari 1995). The combination of the two previous effects finally leads to an increase in the polarisation spectrum for small ℓ, and a decrease for large ℓ, as illustrated in Fig. 5. This behaviour has been previously documented and expounded upon in Zahn & Zaldarriaga (2003). The characteristic scale, ℓ^*, separating these two regimes is approximately $\ell^* \simeq 800$. We note than an equivalent feature exists in the TE spectrum (although it is not represented here). To investigate this further, we conducted separate studies, one focusing solely on the low-ℓ portion of the CMB spectrum ($\ell < \ell^*$) and another centred on the high-ℓ portion ($\ell > \ell^*$), as elaborated upon in the following section. For this ℓ-dependency constraint, we used Planck 2018 data instead of the latest PR4 data (since the decomposition in low ℓ and high ℓ is not yet available in the PR4 likelihood).

3. Results

We used a modified version of the public Boltzmann code CLASS (Blas et al. 2011) to generate temperature and polarisation power spectra that depend on the value of G. The code is publicly available[1]. In addition, we took into account the modification of the primordial helium fraction $Y_{\rm He}$ produced during the BBN phase. This modification was achieved by adapting the PArthENoPE code (Gariazzo et al. 2022). Subsequently, we conducted a Monte Carlo Markov chain (MCMC) analysis employing the ECLAIR code (Ilić et al. 2021; Foreman-Mackey et al. 2013) with its default parametrisation (including the so-called "minimal" neutrino scenario[2]) to fit our model to the latest Planck PR4 data (Tristram et al. 2024), including the latest lensing signal from Carron et al. (2022). More precisely, we used the likelihoods Hillipop TTTEEE, Lollipop low-ℓ E, PR4 lensing, and Commander for low TT (from P18) in combination with data from the BAO from DESI (DESI Collaboration 2025). In some places in the paper, we also use the latest SDSS consensus in order to compare with DESI. It is composed of the main galaxy sample (MGS) from DR7 (Ross et al. 2015) and luminous red galaxies (LRG) from the DR12 (Alam et al. 2017) and DR16 releases: emission line galaxies (ELGs; Raichoor et al. 2020), luminous red galaxies (LRGs; Gil-Marín et al. 2020), Lyman-α forest measurements (LYA; du Bourboux et al. 2020), and quasars (QSOs; Hou et al. 2020), in addition to data from the 6dF survey (Beutler et al. 2011).

The measurements of λ_G using different datasets and models are summarised in Table 1. For the baseline ΛCDM model, we obtain:

$$G = \lambda_G^2 G_{\rm codata} = (6.75 \pm 0.12) \times 10^{-11}\ {\rm m^3\ kg^{-1}\ s^{-2}}, \quad (2)$$

which corresponds to a 1.8% measurement of G, in accordance with the CODATA value (Tiesinga et al. 2021) within 1σ confidence interval. Notably, the precision is more than twice better than the one achieved with Planck 2015 (Bai et al. 2015), and nearly ten times more precise than that obtained with WMAP (Galli et al. 2009). It is also ∼40% better than the precision obtained with Planck 2018 + BAO (see e.g., Wang & Chen 2020). However, this level of precision still falls short of the ultimate, variance-limited measurement of G via the CMB, projected to be 0.4%, according to forecasts presented in Galli et al. (2009). This suggests the potential for enhancement through forthcoming generations of CMB missions (Ballardini et al. 2022). A summary of recent cosmological constraints on G using high-redshift probes is provided in the whisker plot of Fig. 6.

It is worth noting that neglecting the PArthENoPE correction for the BBN would not change the conclusion substantially; it would simply increase the uncertainty in the determination of G. As an illustrative example, for P20 only, we would obtain $\lambda_G = 1.010 \pm 0.013$ without the BBN correction, instead of $\lambda_G = 1.007 \pm 0.011$ with the BBN correction taken into account (see Table 1).

Upon examination of Table 1 and Fig. 7, we observe that the BAO data have a modest impact on the constraint for λ_G. They

[1] https://github.com/yacobozdalkiran/CLASS_mod
[2] i.e. only one massive neutrino of mass 0.06 eV.

Table 1. Constraints on a cosmological measurement of $G = \lambda_G^2 G_{\rm codata}$ for different data combination and cosmological models.

Model	Data	λ_G	H_0 (km s^{-1} Mpc^{-1})	w_0	w_a	Ω_k
ΛCDM	P20 TTTEEE + BAO SDSS	–	67.74 ± 0.41	–	–	–
ΛCDM	P20 TTTEEE + BAO DESI	–	68.22 ± 0.39	–	–	–
$\lambda_G\Lambda$CDM	P20 TT	$1.048^{+0.027}_{-0.035}$	$74.4^{+3.7}_{-5.2}$	–	–	–
$\lambda_G\Lambda$CDM	P18 TT + low E	0.998 ± 0.018	66.9 ± 2.00	–	–	–
$\lambda_G\Lambda$CDM	P18 TT + low E high-ℓ	$0.969^{+0.052}_{-0.058}$	$62.0^{+3.9}_{-4.9}$	–	–	–
$\lambda_G\Lambda$CDM	P18 TT + low E low-ℓ	$1.18^{+0.13}_{-0.038}$	$80.9^{+8.5}_{-4.4}$	–	–	–
$\lambda_G\Lambda$CDM	P20 EE	$1.062^{+0.052}_{-0.059}$	$74.7^{+5.4}_{-6.2}$	–	–	–
$\lambda_G\Lambda$CDM	P20 TE	1.023 ± 0.047	70.5 ± 4.4	–	–	–
$\lambda_G\Lambda$CDM	P20 TTTEEE	1.007 ± 0.011	68.3 ± 1.1	–	–	–
$\lambda_G\Lambda$CDM	P20 TTTEEE + BAO DESI	1.010 ± 0.011	69.11 ± 0.98	–	–	–
$\lambda_G\Lambda$CDM	P20 TTTEEE + BAO DESI + BBN	1.0056 ± 0.0091	68.63 ± 0.87	–	–	–
$\lambda_G w_0$CDM	P20 TTTEEE + BAO DESI	1.008 ± 0.011	$70.8^{+1.7}_{-1.9}$	$-1.070^{+0.062}_{-0.055}$	–	–
$\lambda_G w_0 w_a$CDM	P20 TTTEEE + BAO DESI	1.006 ± 0.011	64.9 ± 3.5	$-0.46^{+0.31}_{-0.42}$	$-1.67^{+1.2}_{-0.79}$	–
$\lambda_G\Omega_k\Lambda$CDM	P20 TTTEEE + BAO DESI	1.008 ± 0.011	69.3 ± 1.0	–	–	0.0016 ± 0.0015

Notes. The first two lines are obtained by fixing $\lambda_G = 1$ in our code, giving consistent results with the literature.

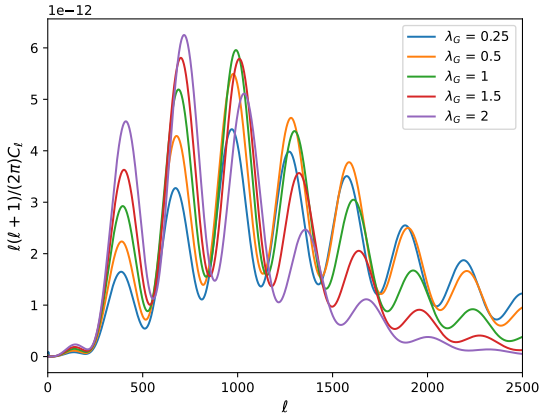

Fig. 5. Effect of λ_G on the EE polarisation power spectrum of the CMB. The same physical energy densities have been used for each curve. When λ_G increases, large ℓ are more damped while small ℓ are less damped than the $\lambda_G = 1$ case.

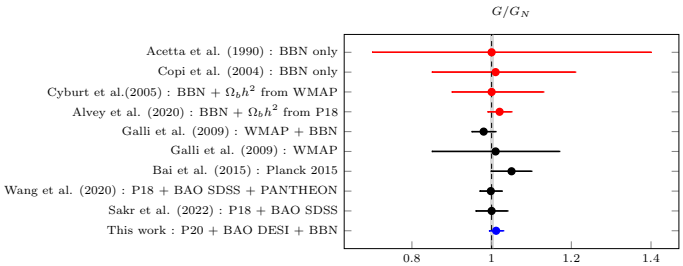

Fig. 6. Recent constraints on cosmological measurements of $G/G_{\rm codata}$ using high-redshift probes. The dashed vertical line corresponds to $G = G_{\rm codata}$, while the light gray area corresponds to an ultimate cosmic-variance-limited precision that could be obtained with the CMB according to Galli et al. (2009).

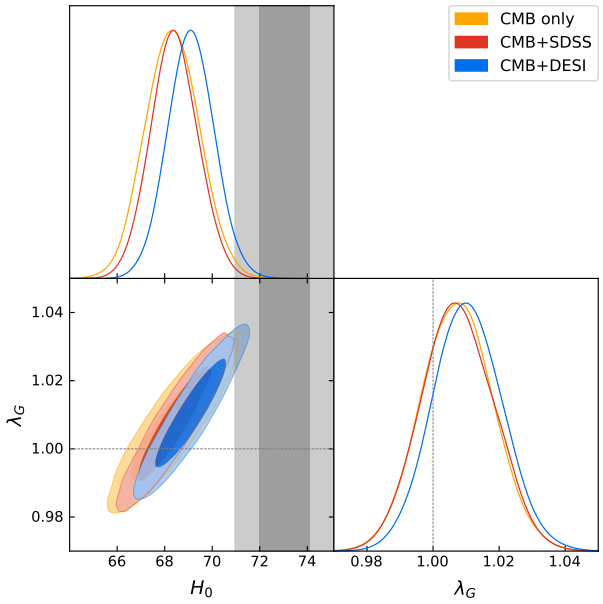

Fig. 7. Constraints and correlation between λ_G and H_0 with CMB+BAO data. The constraint on λ_G is only marginally improved when adding the BAO. The DESI BAO slightly shift the central value of H_0 towards higher values, leading to a moderate 2.8σ tension with the local measurements of H_0 indicated by the vertical grey line (Riess et al. 2022).

marginally nudge λ_G closer to unity while slightly reducing its uncertainty. Figure 7 also reveals a correlation between λ_G and the Hubble constant H_0, highlighting a connection between the gravitational constant and the Hubble constant. Nevertheless, as it can be seen from Fig. 7, a modified value of G at cosmological scales cannot fully resolve the Hubble tension (Verde et al. 2019), even tough the tension decreases to 2.8σ due to a slight increase in the central value of H_0 as well as an increase by a factor ~2 of the uncertainty. This result is consistent with previous studies in the literature (Wang & Chen 2020; Sakr & Sapone 2022).

In Table 2, we present the constraints on the main cosmological parameters derived from an analysis using the Planck 2020 dataset only. Notably, the inclusion of the free parameter λ_G primarily contributes to an increase in the uncertainty associated with each parameter when compared to the baseline ΛCDM model.

In order to assess the dependence of the cosmological measurement of G on the choice of the cosmological model, we

Table 2. Constraints on the standard cosmological parameters using Planck PR4 (denoted as P20) for the $\lambda_G\Lambda$CDM and ΛCDM models.

Parameter	$\lambda_G\Lambda$CDM P20	ΛCDM P20
ω_b	0.02264 ± 0.00052	0.02224 ± 0.00013
ω_{cdm}	0.1193 ± 0.0024	0.1188 ± 0.0012
H_0	68.3 ± 1.1	67.66 ± 0.52
τ_{reio}	0.0582 ± 0.0063	0.0580 ± 0.0062
$\ln(10^{10}A_s)$	3.042 ± 0.015	3.040 ± 0.014
n_s	0.9709 ± 0.0063	0.9680 ± 0.0040

Notes. The uncertainty on all cosmological parameters (except A_s and τ_{reio}) are increased with the addition of the free parameter λ_G.

conducted the analysis within various extensions of the ΛCDM framework. The objective is to assess the impact of given hypotheses regarding the cosmological model on the measurement of G. A comprehensive analysis on the correlation between λ_G and the newly introduced parameters lies beyond the scope of this paper. Specifically, we first explored the w_0CDM model, which accommodates a more general description of the dark energy fluid by introducing a free equation of state parameter, $w_0 = p/\rho$. In the context of this $\lambda_G w_0$CDM model, a notable correlation emerges between w_0 and H_0, leading to an increase in the uncertainty associated to H_0 (see Fig. 8, where we also show the difference between the BAO from the SDSS consensus and the BAO from DESI). This correlation is not specific to a varying-G model since it is already present with $\lambda_G = 1$ and has already been noticed in the literature Ade et al. (2016). We also considered the more sophisticated CPL dark energy equation of state $w(z) = w_0 + w_a \frac{z}{1+z}$ (Chevallier & Polarski 2001; Linder 2003), named, $\lambda_G w_0 w_a$CDM model. As it can be seen in Table 1, the constraint on λ_G is not affected by this generalised dark energy equation of state [3]. We can also recover the result that an evolving dark energy is marginally favoured (DESI Collaboration 2025), even when allowing G to vary, as can be seen from Fig. 9. Finally, we considered spatially curved models, where Ω_k serves as a free parameter. For this non-flat model, the inclusion of BAO data is imperative to mitigate significant parameter degeneracies. The outcomes of this study are summarised in the final four rows of Table 1 and indicates that G remains largely unaffected by the assumptions on the cosmological model. As illustrated in Figs. 8, 9, and 10, these additional parameters are consistent with the standard model, indicating no curvature (Ω_k compatible with zero within 1σ, inline with the latest P20 result Tristram et al. (2024)) and a pure cosmological constant ((w_0, w_a) consistent with $(-1, 0)$ within 1σ).

This section concludes with a detailed examination of the distinct constraints derived from various subsets of the CMB data. Notably, as already mentioned earlier, the primary source of constraints on λ_G stems from its interplay with the polarisation data. Specifically, when considering the temperature spectrum (TT) alone or the polarisation spectrum (EE) alone, there is a preference for a larger value of G, which subsequently yields a higher estimate for the Hubble constant, H_0. This preference aligns with the local measurements reported in Riess et al. (2022), as depicted in Fig. 11 and detailed in Table 1. However, those preferences are accompanied by broader uncertainty ranges. The TE spectrum, on the other hand, occupies an intermediate position between the high and low value for H_0 (see Fig. 11 and Table 1). Notably, the preferred value of H_0 with EE alone changed significantly from P18 to P20. Specifically, using P18 data results in $H_0 = 65.1^{+6.8}_{-8.8}\,\mathrm{km\,s^{-1}\,Mpc^{-1}}$ compared to $74.7^{+5.4}_{-6.2}\,\mathrm{km\,s^{-1}\,Mpc^{-1}}$ of P20 (see Table 1). The same is true for the central value of λ_G, going from $0.956^{+0.069}_{-0.087}$ in P18 to $1.062^{+0.052}_{-0.059}$ in P20. The reason why the combination of TT and EE can give a smaller value of H_0 is illustrated in Fig. 11, where the correlation between λ_G and H_0 and the optical depth of reionisation, τ_{reio}, is evident. The intersection of the contours in the (τ_{reio}, H_0) plot for TT and EE explains the low value of H_0. The better determination of this parameter τ_{reio} in the Planck's PR4 analysis enhances the constraining power of combining TT and

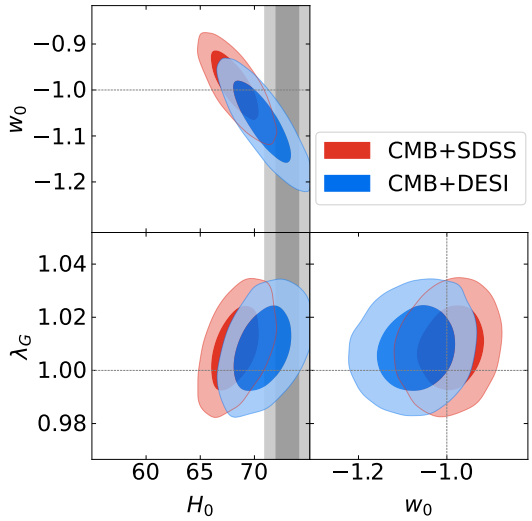

Fig. 8. Constraints on λ_G and w_0 for the $\lambda_G w_0$CDM model. The measurement of H_0 from Riess et al. (2022) is represented as a grey vertical band.

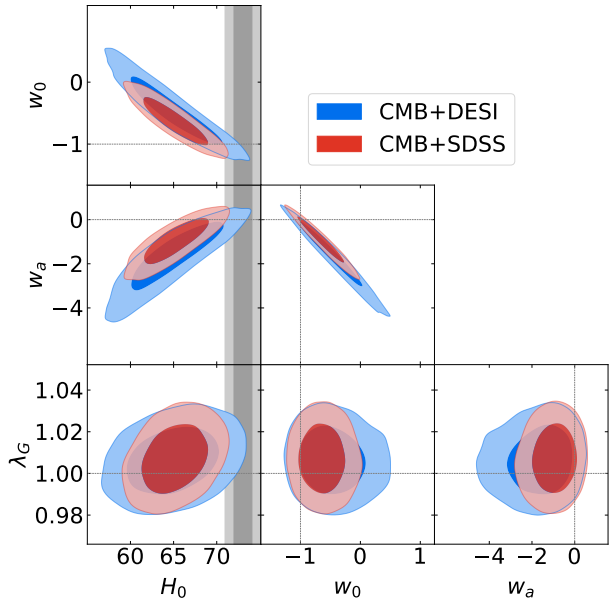

Fig. 9. Constraints on (λ_G, w_0, w_a) for the $\lambda_G w_0 w_a$CDM model. The measurement of H_0 from Riess et al. (2022) is represented as a grey vertical band.

[3] The reason why G is not correlated to w_0 and w_a, as can be seen from Fig. 9, is yet to be investigated in more details in future works.

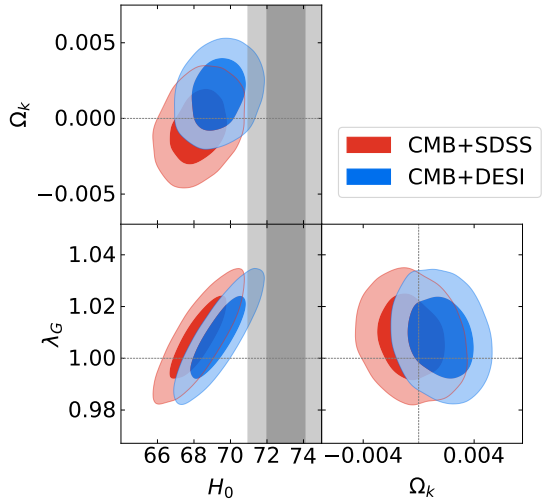

Fig. 10. Constraints on λ_G and Ω_k for the $\lambda_G\Omega_k\Lambda$CDM model. The measurement of H_0 from Riess et al. (2022) is represented as a grey vertical band.

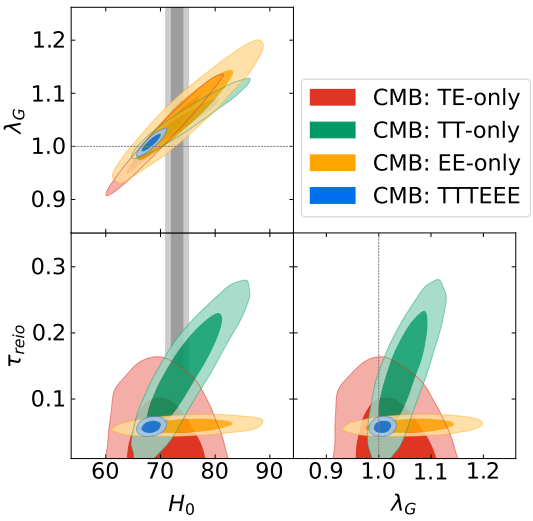

Fig. 11. Influence of different CMB spectra in the constraints and correlation between λ_G and H_0. Note: Commander is used for TT-only, Lollipop for EE-only, and Hillipop for TE-only. The measurement of H_0 from Riess et al. (2022) is represented as a grey vertical band.

EE data. A further improved determination of $\tau_{\rm reio}$ is therefore promising for a more precise measurement of G at cosmological scale (see e.g. Montero-Camacho et al. (2024), who proposed a method to improve the determination of the optical depth of reionisation from the cosmology itself). As a conclusion of this paragraph, it is only through the combination of all these distinct CMB data probes that we can achieve a precise measurement of G and obtain a Hubble constant in accordance with the Planck 2020 dataset.

One of the reasons behind the poor constraint obtained from the TT spectrum lies in the presence of degeneracies with other cosmological parameters that can mimic the same physical effect as a modification of G; namely, altering the damping for large ℓ. It turns out that a combination with only the lowE part of the polarisation spectrum data can already help break these degeneracies. In more details, the combination TT+lowE data greatly enhances the determination of cosmological parameters and, in

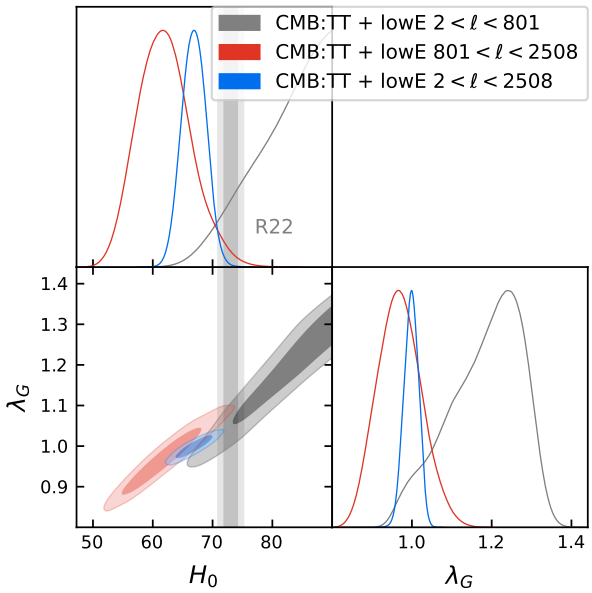

Fig. 12. High-ℓ versus low-ℓ constraints and correlation between λ_G and H_0 when using only the temperature spectrum of Planck 2018. Note: the analysis is done with Planck 2018, for which the likelihoods divided in ℓ are available. The vertical grey band correspond to the Riess value (Riess et al. 2022).

particular, a factor of two on λ_G, as demonstrated in Table 1 and Fig. 12 (where the blue curve represents the TT+lowE part of the Planck 2018 data).

Within the TT+lowE subset of the CMB data, it is instructive to distinguish between the contributions from low-ℓ ($\ell < \ell^*$) and the high-ℓ part ($\ell > \ell^*$) since the effect of λ_G is different on the small and high scales, as discussed in Sect. 2. Notably, the high-ℓ values exhibit more pronounced damping with increasing G and the low-ℓ part is relatively insensitive to variations in G (or can at least be absorbed by adjusting the initial amplitude of the matter power spectrum, as discussed in Sect. 2). It is therefore unsurprising that the constraint on λ_G is significantly degraded when considering the low-ℓ data only. This low-ℓ part tends to favour a higher value of λ_G and consequently this also results in a higher determination of H_0, as depicted in Fig. 12. On the other hand, when focusing on the high-ℓ part of the spectrum, a similar outcome is observed, but this time with a preference for a smaller value of λ_G and a lower estimate for H_0. Finally, we note that even within the ΛCDM model, there is a well-known discrepancy between the low-ℓ and high-ℓ portions in terms of the derived value for H_0. However, this discrepancy is typically considered to be insignificant enough to be deemed problematic (Planck Collaboration Int. LI 2017). Nevertheless, within the λ_G model, this inconsistency becomes even larger and should be investigated within the latest PR4 data release.

4. Conclusion

In this paper, we demonstrate that the impressive precision of cosmic microwave background (CMB) observations allows us to measure the gravitational constant G with a remarkable 1.8% degree of precision. In turns out that this measurement does not depend on model assumptions such as the nature of dark energy or the presence of spatial curvature. Moreover, it is independent from laboratory experiments and probes G on cosmological scales that extend far beyond the reach of laboratory measurements. Our

findings yield a value of $G = 6.75 \pm 0.12 \times 10^{-11}\,\mathrm{m^3\,kg^{-1}\,s^{-2}}$, which aligns seamlessly with laboratory measurements and corresponds to a ∼40% improvement compared to the literature. Most importantly, our study suggests that forthcoming missions, which aim to enhance polarisation measurements (LiteBIRD Collaboration 2023; Abazajian et al. 2019), hold the potential to further refine and bolster this cosmological-scale measurement of G. Finally, we conclude this paper by noting that the constraint obtained on the measurement of the gravitational constant is valid only if G is the sole fundamental constant that varies. The situation differs if, for instance, both G and the fine structure constant α are allowed to vary simultaneously.

Acknowledgements. We thank James Rich for fruitful discussions on the revised version of the paper. We acknowledge use of CLASS (https://github.com/lesgourg/class_public) for calculating power spectra and ECLAIR (https://github.com/s-ilic/ECLAIR) for the sampling of the likelihoods.

References

Abazajian, K., Addison, G., Adshead, P., et al. 2019, ArXiv e-prints [arXiv:1907.04473]
Accetta, F. S., Krauss, L. M., & Romanelli, P. 1990, Physics Letters B, 248, 146
Ade, P. A. R., Aghanim, N., Arnaud, M., et al. 2016, A&A, 594, A13
Ade, P., Aguirre, J., Ahmed, Z., et al. 2019, JCAP, 2019, 056
Alam, S., Ata, M., Bailey, S., et al. 2017, MNRAS, 470, 2617
Alvey, J., Sabti, N., Escudero, M., & Fairbairn, M. 2020, European Physical Journal C, 80, 148
Anderson, J. D., Schubert, G., Trimble, V., & Feldman, M. R. 2015, Europhysics Letters, 110, 10002
Bai, Y., Salvado, J., & Stefanek, B. A. 2015, JCAP, 2015, 029
Ballardini, M., Finelli, F., & Sapone, D. 2022, JCAP, 2022, 004
Bambi, C., Giannotti, M., & Villante, F. L. 2005, Phys. Rev. D, 71, 123524
Benson, B. A., Ade, P. A. R., Ahmed, Z., et al. 2014, in Millimeter, Submillimeter, and Far-Infrared Detectors and Instrumentation for Astronomy VII, SPIE, 9153, 552
Bertschinger, E., & Zukin, P. 2008, Phys. Rev. D, 78, 024015
Beutler, F., Blake, C., Colless, M., et al. 2011, MNRAS, 416, 3017
BIPM 2019, Le Système international d'unités / The International System of Units ('The SI Brochure') (Bureau international des poids et mesures)
Blas, D., Lesgourgues, J., & Tram, T. 2011, JCAP, 2011, 034
Braglia, M., Ballardini, M., Emond, W. T., et al. 2020, Phys. Rev. D, 102, 023529
Brans, C., & Dicke, R. H. 1961, Physical Review, 124, 925
Carron, J., Mirmelstein, M., & Lewis, A. 2022, JCAP, 2022, 039
Chan, K. C., & Chu, M.-C. 2007, Phys. Rev. D, 75, 083521
Chevallier, M., & Polarski, D. 2001, International Journal of Modern Physics D, 10, 213
Copi, C. J., Davis, A. N., & Krauss, L. M. 2004, Phys. Rev. Lett., 92, 171301
Cyburt, R. H., Fields, B. D., Olive, K. A., & Skillman, E. 2005, Astroparticle Physics, 23, 313
Dent, T., Stern, S., & Wetterich, C. 2007, Phys. Rev. D, 76, 063513
DESI Collaboration (Adame, A., et al.) 2025, JCAP, 2025, 021
Di Valentino, E., Melchiorri, A., & Silk, J. 2020, Nature Astronomy, 4, 196
du Bourboux, H., Rich, J., Font-Ribera, A., et al. 2020, ApJ, 901, 153
Fixler, J. B., Foster, G. T., McGuirk, J. M., & Kasevich, M. A. 2007, Science, 315, 74
Fixsen, D. J. 2009, ApJ, 707, 916
Foreman-Mackey, D., Hogg, D. W., Lang, D., & Goodman, J. 2013, PASP, 125, 306
Galli, S., Melchiorri, A., Smoot, G. F., & Zahn, O. 2009, Phys. Rev. D, 80, 023508
Garcia-Berro, E., Kubyshin, Y., Loren-Aguilar, P., & Isern, J. 2006, International Journal of Modern Physics D, 15, 1163
Gariazzo, S., de Salas, P. F., Pisanti, O., & Consiglio, R. 2022, Computer Physics Communications, 271, 108205
Gaztañaga, E., García-Berro, E., Isern, J., Bravo, E., & Domínguez, I. 2001, Phys. Rev. D, 65, 023506
Gil-Marín, H., Bautista, J. E., Paviot, R., et al. 2020, MNRAS, 498, 2492
Greene, K., & Cyr-Racine, F.-Y. 2023, JCAP, 2023, 065
Handley, W. 2021, Phys. Rev. D, 103, L041301
Hou, J., Sánchez, A. G., Ross, A. J., et al. 2020, MNRAS, 500, 1201
Hu, W., Sugiyama, N., & Silk, J. 1997, Nature, 386, 37
Ilić, S., Kopp, M., Skordis, C., & Thomas, D. B. 2021, Phys. Rev. D, 104, 043520
Ivanov, M. M., Ali-Haïmoud, Y., & Lesgourgues, J. 2020, Phys. Rev. D, 102, 063515
Jordan, P. 1959, Zeitschrift fur Physik, 157, 112
Joyce, A., Jain, B., Khoury, J., & Trodden, M. 2015, Physics Reports, 568, 1
Linder, E. V. 2003, Phys. Rev. Lett., 90, 091301
LiteBIRD Collaboration (Allys, E., et al.) 2023, Progress of Theoretical and Experimental Physics, 2023, 042F01
Montero-Camacho, P., Li, Y., & Cranmer, M. 2024, ArXiv e-prints [arXiv:2405.13680]
Mould, J., & Uddin, S. A. 2014, Proc. Astron. Soc. Aust., 31
Nagata, R., Chiba, T., & Sugiyama, N. 2004, Phys. Rev. D, 69, 083512
Olive, K. A. 2021, ArXiv e-prints [arXiv:2105.04461]
Ooba, J., Ichiki, K., Chiba, T., & Sugiyama, N. 2017, Progress of Theoretical and Experimental Physics, 2017
Peracaula, J. S., Gómez-Valent, A., de Cruz Pérez, J., & Moreno-Pulido, C. 2020, Classical and Quantum Gravity, 37, 245003
Planck Collaboration VI 2020, A&A, 641, A6
Planck Collaboration Int. LI. 2017, A&A, 607, A95
Raichoor, A., de Mattia, A., Ross, A. J., et al. 2020, MNRAS, 500, 3254
Riazuelo, A., & Uzan, J.-P. 2002, Phys. Rev. D, 66, 023525
Rich, J. 2015, A&A, 584, A69
Riess, A. G., Yuan, W., Macri, L. M., et al. 2022, ApJ, 934, L7
Ross, A. J., Samushia, L., Howlett, C., et al. 2015, MNRAS, 449, 835
Ruchika, R. H., Choudhury, S. R., & Rentala, V. 2024, JCAP, 2024, 056
Sakr, Z., & Sapone, D. 2022, JCAP, 2022, 034
Tiesinga, E., Mohr, P., Newell, D., & Taylor, B. 2021, Reviews of Modern Physics, 93, 025010
Tristram, M., Banday, A. J., Douspis, M., et al. 2024, A&A, 682, A37
Umezu, K.-I., Ichiki, K., & Yahiro, M. 2005, Phys. Rev. D, 72, 044010
Uzan, J.-P. 2003, Reviews of Modern Physics, 75, 403
Uzan, J.-P. 2011, Living Rev. Relativ., 14, 2
Verde, L., Treu, T., & Riess, A. G. 2019, Nature Astronomy, 3, 891
Wang, K., & Chen, L. 2020, The European Physical Journal C, 80, 570
Wright, B. S., & Li, B. 2018, Phys. Rev. D, 97, 083505
Xue, C., Liu, J.-P., Li, Q., et al. 2020, National Science Review, 7, 1803
Zahn, O., & Zaldarriaga, M. 2003, Phys. Rev. D, 67, 063002
Zaldarriaga, M., & Harari, D. D. 1995, Phys. Rev. D, 52, 3276
Zhao, W., Wright, B. S., & Li, B. 2018, JCAP, 2018, 052